

A STUDY OF RADAR ECHO CLUSTERS OVER SOUTHEASTERN MONTANA

L. Ronald Johnson and Mark R. Hjelmfelt  
Institute of Atmospheric Sciences  
South Dakota School of Mines and Technology  
501 East St. Joseph Street  
Rapid City, South Dakota 57701-3995

**Abstract.** Data recorded by the Skywater radar during the Cooperative Convective Precipitation Experiment were used to produce echo cluster statistics. The average echo cluster is initiated in the mid-afternoon (15:18 MDT) and continues for 1.8 hours. It has a maximum reflectivity of 45.4 dBz, and produces 296 km<sup>2</sup>-mm of rainfall. The storm moves from the west to east at a speed of 12.5 m/s. Analysis revealed a bimodal distribution of maximum echo heights with the low mode at 6.9 km and the upper mode at 9.4 km. Comparison of predictors for radar estimated rainfall confirmed the value of the Area-Time-Integral (ATI). Echo statistics were in good agreement with those obtained from a different project in North Dakota for the same year, with greater differences obtained for statistics from projects in more humid climates. The importance of year-to-year variability is affirmed.

1. INTRODUCTION

During the course of the 1981 Cooperative Convective Precipitation Experiment (CCOPE) centered at Miles City, Montana, a wealth of data was accumulated by many investigators interested in precipitation-producing convective weather systems and beneficial modification of those systems. From these data, many studies have been conducted. Reports have included case studies, moisture budgets, and time histories (Fankhauser et al., 1985; Dye et al., 1986; Koch et al., 1988; Knight and Knupp, 1986; Miller et al., 1988; Rasmussen and Heymsfield, 1987; and Schmidt and Cotton, 1989). Beyond the case studies of particular events that occurred during the field season, few investigators have studied statistical aspects of echo clusters utilizing the existing radar data. This study was accomplished to prepare a composite description of the echo clusters observed in CCOPE. Such a composite should be useful in the comparison of southeastern Montana convective climatology to that of other areas, and to provide a useful data base. Consideration of these results in the design of future weather modification projects for the region should prove beneficial.

The results of the present study can be placed in a broader geographical context by comparison with similar studies performed in other parts of the country. Smith et al. (1985) presented a study of radar echoes observed in western North Dakota during the summers of 1981 and 1982 as a part of the North Dakota Cloud Modification Project. Their results provide a basis for comparisons with nearby data during the CCOPE season and also provide information on year-to-year variability. The motion of radar echo clusters over the Black Hills of South Dakota was studied by Kuo and Orville (1973). Dennis et al. (1971) reported on radar observations of hailstorms in western Nebraska. Foote et al. (1979) presented data on radar cells observed in the National Hail Research Experiment (NHRE) in northeast Colorado, southeast Wyoming, and western Nebraska. These

two studies provide comparisons for intense storms further south in the High Plains. Huff (1987) statistically analyzed data collected on radar storm echoes in Illinois. This study is especially interesting as it provides a contrast between storms observed in the northern Great Plains with those in the more moist Midwest. His study was directed to applications to weather modification, and we will draw upon his results at several points in our discussion.

Results of data collected near St. Louis during the Metropolitan Meteorological Experiment (METROMEX) are summarized in Braham (1981). This study provides results on a slightly different population at the southern edge of the area covered in Huff's (1987) study. Lopez et al. (1984) stratified data on Florida rainstorms in several different categories. Some statistics of storms of similar lifetimes to those observed in the present study are presented.

2. DATA SOURCE AND PROCESSING

For this study, all volume scans recorded by the Skywater radar located near the Miles City airport during CCOPE were acquired. The data set begins with 20 May and continues through 6 August. A typical data recording day started at 1000 local time (all times given are local daylight time) and continued as long as echoes were present or until 2300, whichever occurred first. On 17 July, recording started at 0900; this first hour of collected data is intentionally left out of studies based on time of day.

The Skywater radar operated at a frequency of 5.55 GHz, a pulse repetition frequency of 414 Hz, and a pulse duration of 2  $\mu$ sec with a horizontal beamwidth of 0.9° and a vertical beamwidth of 1°. The radar was located at latitude 46:24:46 north and longitude 105:55:13 west at an altitude of 802.6 MSL. The data bin width along the radial was one-half kilometer. In the volume scan mode, the first complete azimuth scan covered one rotation in 1° azimuth steps at 1° elevation.

The elevation was then increased in 1° increments to a maximum of 12° with a complete rotation at each elevation step. The volume scans were repeated at approximately 5-minute intervals. The data were provided by the U.S. Bureau of Reclamation in the A-file format (Schroeder and Klazura, 1978). A software procedure applied the calibrations that accompanied the requested tapes and compressed the resulting data into reflectivity files. Compression included removal of blue sky and other regions with echoes less than the threshold value (typically 6 dBz). The compressed reflectivity or "dBz" files were used for all succeeding processing.

The first product derived from the dBz file was a CAPPI-like product called "low tilt." It combines the 3° elevation scan from 20-50 km range with the 1° elevation scan for ranges beyond 50 km. Data within a 20 km radius of the radar site were eliminated to minimize ground clutter effects. Data beyond 200 km were also eliminated for the purpose of minimizing range effects. Using the low-tilt product from each volume scan, an echo cluster was defined as one or more contiguous bins with echo meeting the criteria indicated in the next paragraph. The identified cloud cluster commenced at the earliest scan time possible and was followed until dissipation. The cluster was "boxed" by defining range and azimuth coordinates for box corners that enclosed the cluster. The boxing information is used as input into another software utility which derives specific parameters related to volume and area as illustrated in Table 1.

Clusters were chosen when they met specific criteria: 1) the cluster had to be present during

four consecutive scans, or exist for at least 30 minutes; 2) maximum reflectivities had to equal or exceed 25 dBz; 3) the cluster lifetime had to be contained within the radar surveillance area; and 4) if the cluster passed over the 20 km blanked area around the radar during its lifetime, it was dropped from further consideration. Echo splits occurred occasionally in the data set and, when they did, the original cluster identification was maintained for that portion of the echo that continued on the path nearest that of the original cluster. This portion usually exhibited the larger echo area. A new cluster designation was established for the other portion derived from the split if it continued as an entity for the required 30 minutes with reflectivities > 25 dBz. In the event that a small portion split from the main cluster and subsequently decayed within the 30-minute time frame, this portion was included as part of the original cluster. Echo mergers occurred as well; the dominant cluster involved in the merger was considered as the continuing cluster, with the other merging cluster's lifetime ending at the time of merger.

Clusters which drifted into the radar surveillance area as a mature or decaying event were eliminated from the data set. Clusters with initial echo locations at the outer range limit of surveillance were eliminated. Figure 1 shows a slight depression in the number of clusters at maximum range due to this correction. The final data set consisted of 765 clusters.

A broad spectrum of echo size is represented by the studied clusters which range from isolated, one-cell events to multicellular events as large as mesoscale convective systems. No attempt was made to subdivide the cluster set by synoptic type or evolution characteristic such as line, area, or isolated echo. Huff (1987) found little evidence

TABLE 1 Parameters Defined from Each Cluster Lifetime	
PARAMETER	DESCRIPTION
ID	A two character code assigned uniquely each day to identified clusters.
Time	Time of initial scan of the cluster.
Month, Day	Date of initial scan.
DOY	Day of year
Average Reflectivity	Average of the maximum reflectivity of each scan over the cluster's lifetime.
Average Height	Average of the maximum height of each scan over the cluster's lifetime.
Maximum Reflectivity	Maximum reflectivity for the cluster lifetime.
Maximum Height	Maximum height reached by the cluster during its lifetime.
ATI	Area-Time-Integral
Duration	Time difference between initial and final scan.
RERV	Radar estimated rain volume as computed by Z-R relationship.
Range	Average cluster distance from the radar for its lifetime.
Initial Range Initial Azimuth	Coordinates of the cluster first echo.
Surface 850 mb 700 mb 500 mb	
	Wind direction determined from the nearest sounding in space and time for the indicated levels.

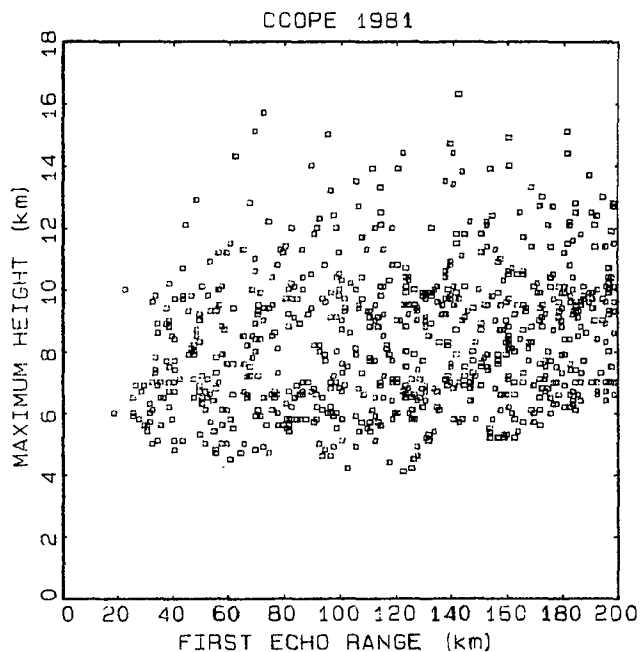


Fig. 1: Scatter plot of cluster lifetime maximum echo height as a function of first echo range ( $r = 0.22$ , slope = 0.010).

to distinguish differences by synoptic type for radar echoes studied from Illinois. A large portion of the CCOPE echoes either had their initiation in a line formation or their initiation helped form a line. Even though all forms of cluster initiation were grouped in this study, it is interesting to note that the average cluster area (168 km<sup>2</sup>) compares with 104 km<sup>2</sup> reported by Huff (1987) for echoes with durations > 15 minutes.

Echo summary outputs provide several parameters; those parameters appear in Table 1. Maximum echo height is determined by the midpoint height (MSL) of the radar bin volume for the bin of greatest height with reflectivity > 20 dBz. Earth curvature and atmospheric refraction are included in the height calculation. The Area-Time-Integral is determined by multiplying the area enclosed by the 25 dBz contour by the centered time interval between the previous and the following scan. For the first scan, the time interval is one-half of the time increment between the initial scan and second scan; for the final increment, it is one-half the period between the last two scans. The product of area > 25 dBz and time is summed over the lifetime of the cluster; the sum is the Area-Time-Integral (Doneaud et al., 1984). Parameter RERV is the radar estimated rain volume as computed by using a Z-R relationship ( $Z = 155R^{1.88}$ , Smith et al., 1975). A rain rate is determined for each reflectivity recorded at the low-tilt elevations. The rain rate is multiplied by the projected area of the radar range bin and the time increment between scans. The product is summed for all bins for each scan for the lifetime of the cluster to get rain volume for the event.

The last four entries of the table are derived from soundings and are wind speeds based on soundings from one of six stations (Miles City, Baker, Colstrip, Knowlton, Powderville, and Glendive). The selected sounding was taken nearest in time (preceding the first echo time) and position to that of the cluster first echo. Wind directions at the surface, 850 mb, 700 mb, and 500 mb were included in the data set.

The range was bounded by a minimum of 20 km to a maximum of 200 km. Consideration of the beam characteristics implies that the nearest bin had a projected area of 0.18 km<sup>2</sup>, while the most distant had a 1.74 km<sup>2</sup> projected area. This difference could be reflected in the data set as a range bias. From the radar parameters that were selected, maximum height is one of the parameters that should be influenced by a range bias.

The scatter plot of maximum echo height as a function of first echo range is presented in Fig. 1 to demonstrate a possible range bias. This figure indicates lower maximum heights in the 20 to 80 km range. This would indicate that the actual tops of the storms were not observed in this range interval because of the restricted scan elevations. At 12° elevation and 80 km range, the greatest echo height possible is 17.8 km, which is beyond the observed upper limit. For ranges greater than 140 km, the smaller events are missed; at maximum range, cloud tops must exceed 6.6 km to be observed. Echoes at long ranges require more development before satisfying the threshold because reflectivities for the larger

bin volumes represent an average value for the total volume. This effect is substantiated by maximum reflectivity observations as well. Reflectivities do not exceed 60 dBz for ranges > 160 km; near 200 km, the maximum limit is nearer 55 dBz. For the parameters selected for study, only height will be directly affected by the bias at shorter ranges. Storm size (ATI, RERV, duration, and height) will average slightly above the true mean for large ranges. With these biases in mind, the following results are reported.

### 3. TYPICAL ECHO CLUSTER CHARACTERISTICS

Histograms of selected parameters are displayed in Figs. 2a-c. The central tendencies for these parameters are illustrated in Table 2. Figure 2a demonstrates the time-of-day frequency for first echo occurrence. The major peak between 1000-1100 occurs because of project design. Skywater radar began operations at 1000 whenever a "go" day was declared. Therefore, the percentage of "first echoes" at 1000 is artificially enhanced because earlier scans were not available and the first echo times were taken as the first scan time if the cluster was still growing. As expected, beyond the 1000 anomaly, the curve is somewhat bell-shaped with maxima occurring in the afternoon and evening. The mean and median of this distribution are the same and occur at 1518, while the mode is the 1000 block.

Frequency of storms as a function of day of the year is demonstrated in Fig. 2b. This histogram blocks the data by five-day segments and illustrates that there is great variability between the five-day groupings. It is interesting that the storms identified as significant events for case study analysis did not always occur during episodes of maximum storm frequency. Frequency extremes range from a low of 1.0% to a maximum of 14.5% and occur back-to-back around 24 July. An unusual event would be an entire five-day block without any storms, while it is not unusual for a five-day block to contain 10% of the summer events.

The typical echo cluster has a lifetime duration of 1.80 hour (distribution mean). Longest duration was over 10 hours. Some storms left the area during their lifetime and were not included in this study. This results in a bias decreasing the numbers of longer lasting storms. For storm motions of 12.5 m/s, durations of 9 hours or more are eliminated. The net effect of this bias is an accelerated frequency depression as a function of duration.

The distribution of maximum heights reached by echo clusters during their lifetimes is presented by Fig. 2c. The distribution is bimodal, centering about 6.9 and 9.4 km. The distribution is skewed to higher levels with 16.3 km being the highest observed. No cases were found to have maximum heights less than 4 km. The bimodal distribution is of interest and has also been observed by Braham (1981) during the METROMEX Project as given by the dashed line in the figure. Based on a numerical cloud model study by Mueller (1978), he attributed the bimodal distribution in cloud heights observed in the rural METROMEX population to the role of glaciation and cloud radius in allowing clouds to grow past mid-level dry layers. Small clouds are more strongly affected by mixing and thus are stopped by dry layers

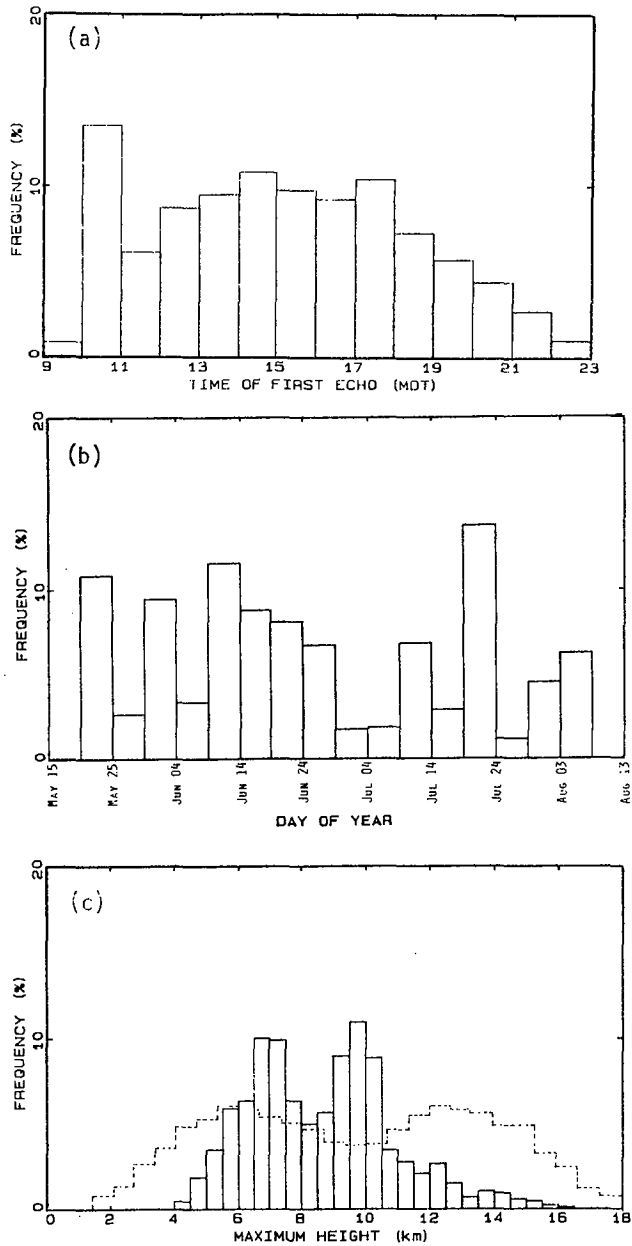


**Fig. 2:** Frequency histograms: a) Time of first echo using 1-hr bins to categorize the data set. On 17 July, operations started at 9:00 a.m., and these data are included in this figure for completeness. b) Occurrence of convective event by day of season using bins 5 days in width. The figure is extended with an empty block before 20 May and after 6 August to increase readability. c) Cluster lifetime maximum echo height using 1/2 km bin width. Dashed line for St. Louis clouds, adapted from Braham (1981).

aloft. Larger clouds are able to protect the updraft core from the effects of mixing with the dry mid-level environment and thereby continue to near the tropopause. Two modes are thus created: A low mode determined by the height of the mid-level dry layer and a high mode which is determined by the height of the tropopause. This may be a plausible hypothesis for the occurrence of the bimodal cloud height distribution in the CCOPE clouds.

	MEAN	MEDIAN	MODE	2 $\sigma$ RANGE	UNITS
Time of Day	15:18	15:18	10:02	12:02-18:34	hr (MDT)
Day of Year	175	170	202	152-199	day
Duration	1.80	1.33	0.51	0.4-3.2	hr
Maximum Height	8.4	8.2	6.9/9.4	6.2-10.6	km
Maximum Reflectivity	45.4	44.4	36.7	36.6-54.0	dBz
Radar Estimated Rain Volume	296†	284	1026	36.4-2406	km <sup>2</sup> ·mm
Area Time Integral	93.6†	80.0	22.4	13.9-628	km <sup>2</sup> ·hr
Average Range	123	125	124	82-164	km
Initial Range	122	125	193	73-171	km
Initial Azimuth	197	211	295	94-330	degree

†Mean of an assumed log normal distribution.

The radar reflectivity maxima (not shown) are distributed about a mean of 45.4 dBz and are skewed to lower values as indicated by a mode of 36.7 dBz. Reflectivities range from the threshold to a maximum of slightly over 67 dBz. About 17% of the cases reached maximum reflectivities exceeding 55 dBz, which has been shown by numerous investigators to be a reasonable indicator of the presence of hail (Dennis et al., 1971; Foote et al., 1979).

Radar rain volume estimates range from 1.1 to 163973 km<sup>2</sup>·mm (km<sup>2</sup>·mm = 1 metric kiloton) with both extreme events occurring on 31 May. The average is 296 km<sup>2</sup>·mm which implies that the typical storm produces little moisture; only 6.3% of the events produced amounts > 10,000 km<sup>2</sup>·mm. Half the total rainfall (922821 km<sup>2</sup>·mm) was produced by 3% of the 765 clusters.

### 3.1 Cluster motion

A companion study of the CCOPE radar data resulted in an M.S. thesis by Tao (1987) which primarily dealt with cluster motion. The results of his study are summarized in Table 3. Mr. Tao's procedure was to subdivide the season into six time periods; this is the vertical presentation of the table. The horizontal extent of the table represents the eight cardinal directions of tracks taken by clusters. The numbers represent the percent of all clusters for a given time period that had trajectories from the given direction. The final table entry is the composite for the season.

The first time period, 20-31 May, indicates that cluster trajectories swept across the CCOPE network from the directions of north through east to southwest with no occurrences moving from the directions west to northwest, the highest frequencies of storm movement being from the southeast and southwest. The speeds were lower in the first period than for the rest of the season. The next time period (1-15 June) demonstrates a dramatic shift with trajectories preferring a west to east movement. This preference continues throughout the season except for the 1-15 July period when the southwest direction was slightly favored.

TABLE 3  
Frequency of the Direction of Cluster Motion†

	No.	N	NE	E	SE	S	SW	W	NW	SPEED (m/s)
May 20-31	146	9	9	7	36	11	28			4-12
Jun 1-15	191					4	29	50	17	12-14
Jun 16-30	169			3	1		14	62	20	11-18
Jul 1-15	102				4	5	62	29		11
Jul 16-31	206						6	84	10	10-11
Aug 1-6	87						26	65	9	12-14
Season		1	1	2	7	3	28	48	9	10-18

†Based on Tao (1987). Motion is from the direction given similar to that used to describe wind direction. Last entry is the season summary.

This dominance of west to east trajectories during the summer months is as expected (Kuo and Orville, 1973). Typical cluster trajectories for the 1981 season are from the southwest or west at a speed of  $12.5 \text{ m s}^{-1}$ . Mean speed is uniform across all time periods except for May when the mean speed was  $7 \text{ m s}^{-1}$ . The transition from winter-spring weather systems to summer weather patterns which occurs near the end of May has a drastic effect on echo-cluster trajectories. This record indicates that this occurred toward late May or early June.

### 3.2 Parametric variation during the day

Several of the parameters were reduced to hourly averages over the course of the project. For example, all measurements of duration for echo clusters that have a start time between 1000-1100 are averaged and illustrated in Fig. 3a by a point at 1000. Continuing this averaging technique for succeeding hours resulted in Fig. 3a. The averages tend toward the 1.8 hour overall mean with shorter durations for echo clusters starting later in the day. By project design, echo clusters starting late cannot have a long measured lifetime, yet storms that begin in the late evening may be inherently small and short-lived. Unfortunately, this comparison is incapable of discrimination between the two causes.

Hourly average maximum height is demonstrated in Fig. 3b. The greatest average maximum height of all echo clusters occurred for events with starting times after 2000 in the evening. There is a tendency for the maximum heights to increase throughout the day with a downward deflection around 1900. It has been documented that there's an early-evening resurgence of activity in this region (Koscielski and Dennis, 1976; Miller and Smith, 1986). The final two points could be contaminated because clusters that lasted longer than the surveillance time could not be included. Maximum reflectivity hourly averages (not shown) scatter about the mean (45.3 dBz), with lower values (43 dBz) for the morning period (1000 to 1200). The highest hourly averages occur in storms that start at 1700 (48.1 dBz) and 2100 (47.7 dBz). The estimated rain per cluster was also averaged by hour and the mean of  $296 \text{ km}^2 \cdot \text{mm}$  is followed by 9 of the 12 hourly intervals; the other 3 intervals (17, 20, 21 hrs) are well

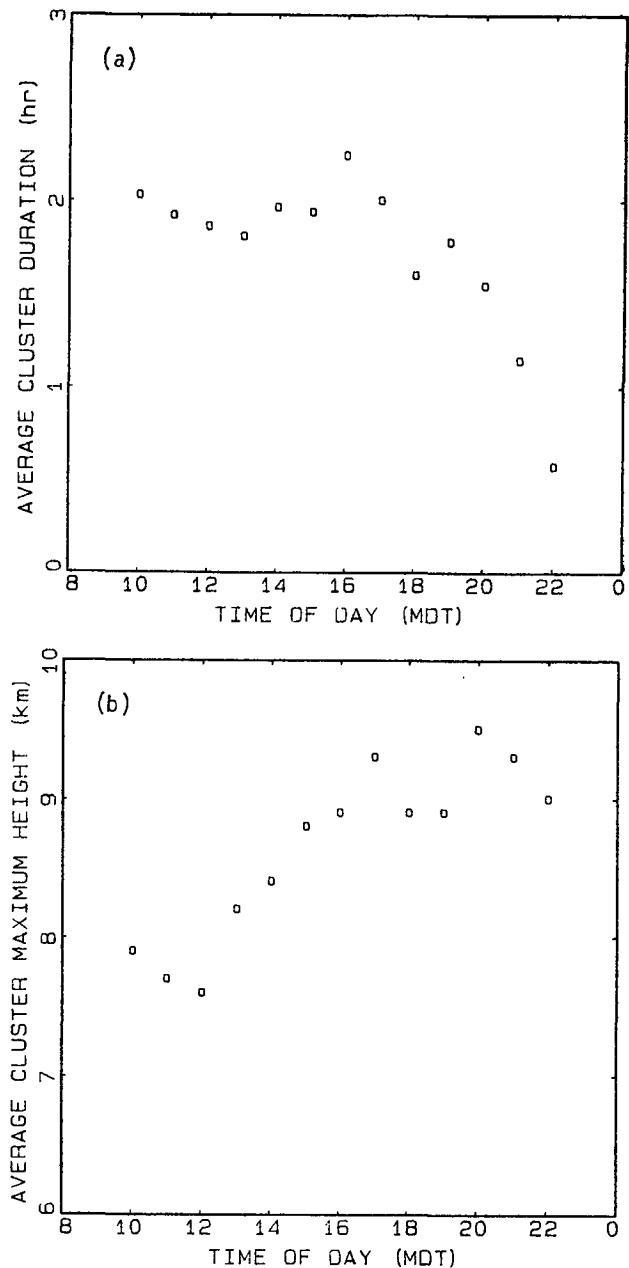


Fig. 3: Project hourly averages plotted against time of day: a) Cluster duration ( $r = -0.71$ ); b) Cluster maximum height ( $r = 0.88$ ).

above this value. Cluster rainfall hourly averages range from a low of  $153 \text{ km}^2 \cdot \text{mm}$  at 1200 to a high of  $638 \text{ km}^2 \cdot \text{mm}$  at 2100. The trend is for larger amounts of rainfall as the day progresses, as indicated by regression which resulted in a slope of  $30.8 \text{ km}^2 \cdot \text{mm/hr}$  ( $r=0.75$ ). Storms that begin in the late afternoon and evening produce the most rain.

### 3.3 Seasonal influence

As previously demonstrated by Fig. 2c, echo cluster maximum height had a wide bimodal distribution with well-defined modes of 6.9 km and 9.4 km. When an average maximum height is considered for each day and plotted as a function of date, Fig. 4 results. Considerable scatter exists, yet there is a tendency for higher clouds

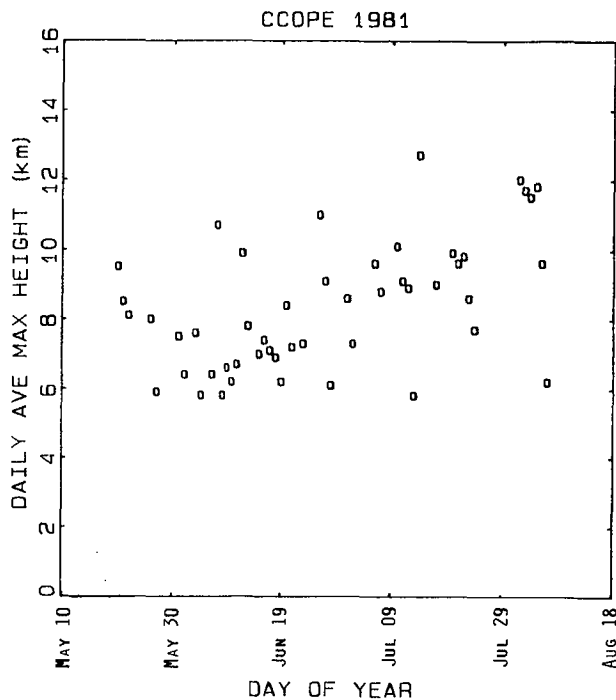


Fig. 4: Scatter plot of daily averaged cluster maximum height against day of year ( $r = 0.51$ , slope =  $0.042$  km/day).

with advancement of the year. The correlation coefficient is  $0.51$  and the slope is  $0.042$  km/day.

Using a similar averaging technique, several other parameters were followed throughout the summer season. The daily averaged echo duration is scattered about the mean with no substantial trend ( $r = -0.16$ , slope =  $-0.004$  h/day). Since echo height increases through the season, it would be suspected that reflectivities would as well. Daily averaged maximum reflectivities result in a correlation of  $0.28$  and a slope of  $0.059$  dBz/day. Radar estimated rain volume daily averages indicate that these later-season storms do not produce a disproportionate amount of rainfall, no tendency is apparent, the correlation being  $0.02$  and the slope  $0.001$   $\text{km}^2 \cdot \text{mm}/\text{day}$ . In summary, events early in the summer last slightly longer and may be less intense than events later in the year. The rainfall per event remains fairly constant throughout the season.

### 3.4 Parameters that influence rainfall

The longer an echo cluster exists, the greater the opportunity for rainfall to occur; duration should therefore be directly correlated to rainfall. Figure 5a demonstrates the scatter plot of duration to radar estimated rain volume (log scale). Indeed, the overall relationship supports this supposition ( $r = 0.75$ ). Yet, when one considers the scatter, an event that lasted only one hour produced a rain volume of close to  $10,000$   $\text{km}^2 \cdot \text{mm}$ , while another echo cluster that existed for an hour produced  $< 10$   $\text{km}^2 \cdot \text{mm}$  of rain. Thus there are huge differences in the absolute quantity of rain that falls for any given duration. There is also a noticeable curvature in the scatter plot suggesting that the relationship is actually nonlinear.

A plot of maximum height versus rain volume is presented in Fig. 5b and, as expected, there is a tendency for taller clouds to produce greater radar estimated rainfall. Maximum height is not a high confidence measure of rainfall, as one cluster with a maximum height of  $> 10$  km yielded  $< 10$   $\text{km}^2 \cdot \text{mm}$  while another event with maximum height of about  $6$  km exceeded  $10,000$   $\text{km}^2 \cdot \text{mm}$  rainfall. Generally, however, the larger rainfall storms are also the taller storms; the statistics yield a correlation of  $0.65$  and a standard log error of  $0.694$ . Another parameter which trends with height is maximum reflectivity. Maximum reflectivity is compared to radar estimated rain volume in Fig. 5c. This results in a correlation of  $0.80$  and a standard log error of  $0.55$ . The indication is that rainfall over the lifetime of the storm is proportional to maximum reflectivity.

Consistently strong correlations have been found for the comparison of ATI to RERV by Doneaud et al. (1984) for data collected during field projects in North Dakota. A similar correspondence was reported by Lopez et al. (1983, 1989) for Florida. The ATI comparison to RERV for CCOPE is presented in Fig. 5d. The relationship is very similar to those found in North Dakota. Using this relation for an estimation of rainfall results in a power law that can be represented by  $V = K \text{ATI}^b$ , where  $V$  = total rain volume, and  $K$  and  $b$  are constants of proportionality to be determined. The values of the multiplier  $K$  and the exponent  $b$  which have been determined for several projects are listed in Table 4. The multiplier  $K$  represents the average rain rate (mm/hr) for all echo clusters for the project. The exponent ( $b$ ) being near one indicates that ATI values are additive, such that rainfall for composite events can be estimated as well.

The data set was subdivided by the 8 cardinal wind directions as a function of 4 heights (or pressures) observed by the proximity soundings at cluster initiation time, for a total of 32 possible categories. The frequency distribution of ambient wind direction at specific heights connected with cluster initiation is demonstrated by Table 5. At the surface, there is an obvious trend for wind directions at initiation time to be west through north and a secondary max for winds from the south. At the  $850$  mb level, the trend is still striking in the west/north sector and a secondary peak exists for south/southeast winds. Going to higher levels, the predominant wind nearly always has a westerly component exhibiting nearly zonal flow.

The possibility of terrain and surface inhomogeneity influences on first echo locations in the CCOPE area has been identified (Smolarkiewicz and Clark, 1985; Auer and White, 1983; Klitch and Vonder Haar, 1982). Further studies are investigating the possible relationship of observed FE locations to topographic features.

## 4. COMPARISONS WITH OTHER STUDIES

Comparison with other studies is made possible by the use of Table 6, which is comprised of average values that have been reported for other projects. One useful comparison would be with data from the North Dakota Cloud Modification Project in 1981. Comparing these two columns, CCOPE had first echoes that started 40 minutes

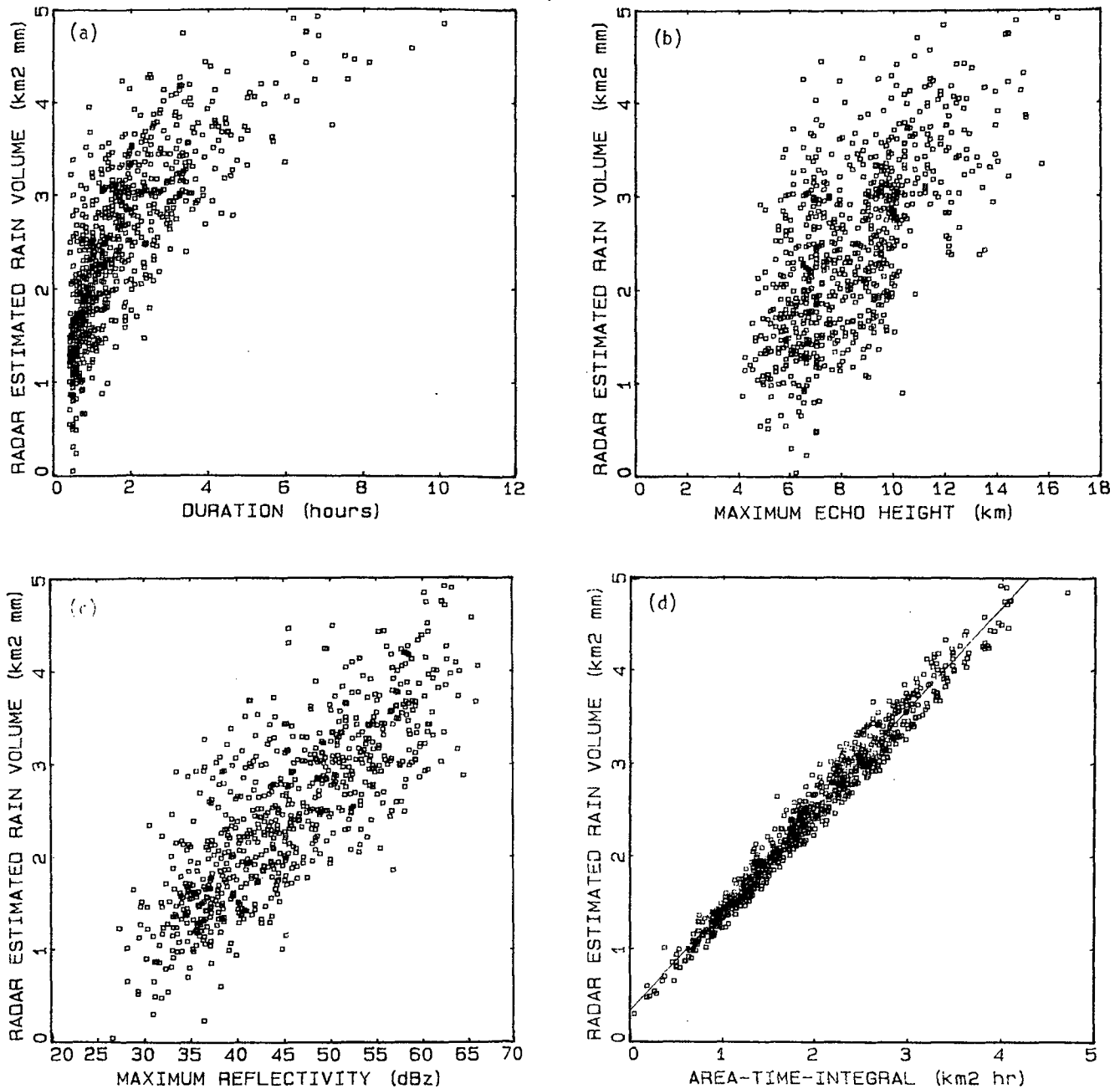


Fig. 5: Scatter plots against the log of radar estimated rain volume: a) Duration ( $r = 0.75$ , slope =  $1.155 \text{ km}^2 \cdot \text{mm/hr}$ ). b) Cluster maximum height ( $r = 0.65$ , slope =  $1.591 \text{ km}^2 \cdot \text{mm/km}$ ). c) Cluster lifetime maximum reflectivity ( $r = 0.80$ , slope =  $7.54 \text{ km}^2 \cdot \text{mm/dBz}$ ). d) Log of Area-Time-Integral ( $r = 0.987$ , slope =  $0.896 \text{ km}^2 \cdot \text{mm/km}^2 \cdot \text{hr}$ ).

earlier than those in North Dakota and lasted about 12 minutes longer. Maximum echo height was 1.4 km lower and maximum reflectivity about the same. The radar estimated rainfall difference of  $54 \text{ km}^2 \cdot \text{mm}$  with ND larger is opposite to that in storm size (CCOPE  $40 \text{ km}^2$  greater in area). Being larger, yet producing less rain, would require the average rain rate be less for CCOPE clouds, and it is by  $1.2 \text{ mm hr}^{-1}$ . The ATI remains comparable.

The North Dakota 1982 comparison shows that CCOPE echo initiation time was 1:40 hours earlier, yet height and maximum reflectivity are much the same. Estimated rain volume is reduced by half

for North Dakota, 1982; this reduction is also seen in the ATI value. Differences between ND 81 and 82 for the same area are greater than differences between CCOPE and ND 81.

Comparison to other projects is not quite as straightforward but is attempted in Table 6. Radar beam characteristics, project surveillance methods, parameter definitions, and reported stratifications are some of the conflicts that arise in such comparisons. Other projects that report a first echo beginning time indicate ~1 hour later initiation. Duration is not as easy to compare as the size criteria for cluster

TABLE 4  
Rainfall Estimation Based on Area-Time-Integral

PROJECT	K (mm/hr)	b	c	RMS LOG ERROR
NDPP-1972†	2.62	1.09	0.97	0.16
NDCMP-1980*	3.68	1.01	0.98	0.17
NDCMP-1981*	3.07	1.08	0.98	0.16
Florida (1979-1981)††	3.4	1.0		
CCOPE-1981	2.133	1.086	0.987	0.147

†Doneaud et al., 1981.  
\*Doneaud et al., 1984.  
††Lopez, 1989.

TABLE 5  
Frequency Distribution (%) of Echo Clusters  
as a Function of Wind Direction at the  
Indicated Height for the Eight  
Cardinal Directions

	N	NE	E	SE	S	SW	W	NW
Surface	23.3	3.7	7.2	7.4	15.3	7.5	13.4	22.1
850 mb	12.7	2.4	6.3	16.0	11.1	6.7	19.0	25.8
700 mb	5.8	0.4	0.4	6.7	12.5	18.4	43.9	11.8
500 mb	4.5	0	3.4	2.5	3.4	21.3	61.8	3.0

definition changed between projects. NHRE and METROMEX report comparable durations of 50 minutes to an hour, while the Illinois projects reported duration of only 25 minutes. Data for Florida echoes lasting 1 hour were chosen for inclusion in Table 6 as most likely to be comparable.

Maximum height appears comparable in most regions, except for the western Nebraska and the NHRE projects, which were designed to study large hailstorms. This is further borne out by the average maximum reflectivity of 57 dBz reported for NHRE. Rain volume estimates vary in the same area from year to year (note North Dakota 1981 and 1982) by a factor of three. It is evident that southeastern Montana and northwestern North Dakota tend to produce less rainfall per event than the Midwest (Illinois and St. Louis). At the same time, the clouds producing the rain in the northern Great Plains are greater in areal extent. Florida demonstrates the smallest clouds in the comparison. Very few average rain rates were available, but the higher rates in Illinois would explain more rain from smaller clouds than seen in the northern Great Plains, as expected from the greater moisture available.

## 5. CONCLUDING REMARKS

In conclusion, we find a general consistency of the results described in this study with those of North Dakota 1981. This suggests that these results are applicable to the broader northern

TABLE 6  
Parametric Mean Value Comparisons with Other Projects

	CCOPE	ND 81	ND 82	ILL	NHRE	ST. LOUIS	NEBR. HAIL	FLA
Initiation Time (hr:min)	15:18	~1600	~1700		1600	1700	1600	
Duration (hr)	1.8	1.5	--	0.4	0.9	0.8		1.0
Max Height (km)	8.4	9.9	8.6	8.6	10.7	8.6	11.4	9.4
Max. Reflec. (dBz)	45	44	41	38	57		45	40
Rain Vol. (km <sup>2</sup> ·mm)	296	350	131	548		1220		
Max Area (km <sup>2</sup> )	168	123		104		114		92
Average Rain Rate (mm/hr)	3.16	4.4	3.5	9				
Depth (mm)							11.4	
ATI (km <sup>2</sup> ·hr)	93.1	80	32.8					
Total Area (km <sup>2</sup> )								815

Great Plains region. We note that the Smith et al. (1985) study indicates the potential for substantial year-to-year variation in echo statistics which is demonstrated by the North Dakota 1981-1982 comparison. This suggests that caution should be used in extrapolation of these results to other years. There are greater differences when compared with radar echoes from more humid environments.

To our knowledge, the bimodal distribution of maximum echo heights observed in the present study has not been reported previously for High Plains storms. The implications of the results of the modeling study by Mueller (1978) suggesting that METROMEX clouds could be moved from the lower mode to the higher mode as a result of enhanced glaciation are especially intriguing.

The usefulness of the Area-Time-Integral (ATI) in estimating total storm rainfall is reaffirmed for this data set. On the other hand, maximum echo height is found not to be as good an estimator of rainfall, as found in previous studies (Smith et al., 1985a, 1985b). Perhaps the better resolution provided by the 1° beamwidth of the Skywater radar data used here is a factor.

Finally, some of the time of day and seasonal trends can be useful in planning weather modification projects in the region.

**Acknowledgments.** Support of this research was provided by the National Science Foundation, Division of Atmospheric Sciences, under Grant ATM-8610159.

Special thanks are extended to Douglas Black, Greg Thesis, and Chris Kruschke for all their tedious efforts in processing the data. Thanks are also extended to Dr. Paul L. Smith for his scientific leadership and to Mrs. Sandra Palmer and Mrs. Joie Robinson for typing the manuscript.



## REFERENCES

- Auer, A. H., and J. M. White, 1983: Boundary layer perturbation associated with terrain, physiographical and topographical influences in CCOPE. Final Report, NSF Grant ATM-8107096, Dept. of Atmospheric Sciences, University of Wyoming. 57 pp.
- Braham, R. R., Jr., 1981: Urban precipitation processes. In METROMEX: A Review and Summary. Meteor. Monogr., Vol. 18, No. 40, 76-116.
- Dennis, A. S., P. L. Smith, Jr., E. I. Boyd and D. J. Musil, 1971: Radar observations of hailstorms in western Nebraska. Report 71-1, Institute of Atmospheric Sciences, S.D. School of Mines and Technology, Rapid City, SD. 42 pp.
- Doneaud, A. A., P. L. Smith, A. S. Dennis and Sumedha Sengupta, 1981: A simple method for estimating convective rain volume over an area. Water Resources Research, 17, 1676-1682.
- Doneaud, A. A., S. Ionescu-Niscov, D. L. Priegnitz and P. L. Smith, 1984: The area-time integral as an indicator for convective rain volumes. J. Climate Appl. Meteor., 23, 555-561.
- Dye, J. E., J. J. Jones, N. P. Winn, T. A. Cerni, B. Gardiner, D. Lamb, R. L. Ritter, J. Hallett and C. P. R. Saunders, 1986: Early electrification and precipitation development in a small, isolated Montana cumulonimbus. J. Geophys. Res., 91, 1231-1247.
- Fankhauser, J. C., C. J. Biter, C. G. Mohr and R. L. Vaughan, 1985: Objective analysis of constant altitude aircraft measurements in thunderstorm inflow regions. J. Atmos. Oceanic Technol., 2, 157-170.
- Foote, G. B., R. E. Rinehart and E. L. Crow, 1979: Results of a randomized hail suppression experiment in northeast Colorado. Part IV: Analysis of radar data for seeding effect and correlation with hailfall. J. Appl. Meteor., 18, 1569-1582.
- Huff, F. A., 1987: Summary of several radar echo studies for weather modification application in Illinois. J. Wea. Modif., 19, 82-91.
- Klitch, M. A., and T. H. Vonder Haar, 1982: Compositing digital satellite data to detect regions of orographically induced convection on the northern High Plains. Paper No. 351, Dept. of Atmospheric Sci., Colorado State University, Fort Collins, CO. 87 pp.
- Knight, C. A., and K. Knupp, 1986: Precipitation growth trajectories in CCOPE. J. Atmos. Sci., 43, 1057-1073.
- Koch, S. E., R. E. Golus and P. B. Dorian, 1988: A mesoscale gravity wave event observed during CCOPE. Part II: Interaction between mesoscale convective systems and the antecedent waves. Mon. Wea. Rev., 116, 2545-2569.
- Kuo, J.-T., and H. D. Orville, 1973: A radar climatology of summertime convective clouds in the Black Hills. J. Appl. Meteor., 12, 359-368.
- Lopez, R. E., J. Thomas, D. O. Blanchard and R. L. Holle, 1983: Estimation of rainfall over an extended region using only measurements of the area covered by radar echoes. Preprints 21st Conf. Radar Meteor., Edmonton, Alberta, Canada, Amer. Meteor. Soc., 681-686.
- Lopez, R. E., D. O. Blanchard, D. Rosenfeld, W. L. Hiscox and M. J. Casey, 1984: Population characteristics, development processes and structure of radar echoes in south Florida. Mon. Wea. Rev., 112, 56-75.
- Lopez, R. E., D. Atlas, D. Rosenfeld, J. L. Thomas, D. O. Blanchard and R. L. Holle, 1989: Estimation of rainfall using the radar echo area time integral. J. Appl. Meteor., 28, 1162-1175.
- Koscielski, A., and A. S. Dennis, 1976: Comparison of first radar echoes in seeded and unseeded convective clouds in North Dakota. J. Appl. Meteor., 15, 309-311.
- Miller, J. R., and P. L. Smith, 1986: Some characteristics of radar first echoes in the High Plains. J. Wea. Modif., 18, 95-101.
- Miller, L. J., J. D. Tuttle and C. A. Knight, 1988: Airflow and hail growth in a severe northern High Plains supercell. J. Atmos. Sci., 45, 736-762.
- Mueller, S. F., 1978: An application of the Simpson-Wiggert cloud model to METROMEX Hi-Cu data. Preprints Conf. Cloud Physics and Atmos. Elec., Issaquah, WA, Amer. Meteor. Soc., 490-495.
- Rasmussen, R. M., and A. J. Heymsfield, 1987: The melting and shedding of graupel and hail: Part III. Investigations of the role of shed drops as hail embryos in the August 1 CCOPE severe storm. J. Atmos. Sci., 44, 2783-2803.
- Schmidt, J. M., and W. R. Cotton, 1989: A High Plains squall line associated with severe surface winds. J. Atmos. Sci., 46, 281-301.
- Schroeder, M. J., and G. E. Klazura, 1978: Computer processing of digital radar data gathered during HIPLEX. J. Appl. Meteor., 17, 498-507.
- Smith, P. L., D. E. Cain and A. S. Dennis, 1975: Derivation of an R-Z relationship by computer optimization and its use in measuring daily areal rainfall. Preprints 16th Radar Meteor. Conf., Houston, TX, Amer. Meteor. Soc., 461-466.
- Smith, P. L., J. R. Miller, Jr., A. A. Doneaud, J. H. Hirsch, D. L. Priegnitz, P. E. Price, K. J. Tyler and H. D. Orville, 1985a: Research to develop evaluation techniques for operational convective cloud modification projects. Report SDSMT/IAS/R-85/02, Institute of Atmospheric Sciences, S.D. School of Mines and Technology, Rapid City, SD. 93 pp.
- Smith, P. L., A. A. Doneaud, J. H. Hirsch, J. R. Miller, Jr., and P. E. Price, 1985b: Development of evaluation techniques for operational convective cloud modification projects: 1984-85 studies. Report SDSMT/IAS/R-85/05, Institute of Atmospheric Sciences, S.D. School of Mines and Technology, Rapid City, SD. 34 pp.
- Smolarkiewicz, P. K., and T. L. Clark, 1985: Numerical simulation of the evolution of a three-dimensional field of cumulus clouds. Part I: Model description, comparison with observations and sensitivity studies. J. Atmos. Sci., 42, 502-522.
- Tao, Ningsheng, 1987: Some radar echo characteristics during CCOPE. M.S. Thesis, Dept. of Meteor., S.D. School of Mines and Technology, Rapid City, SD. 102 pp.